



DETAILED PRESSURE DISTRIBUTION ANALYSIS OF A CONFEDERATION BRIDGE PIER

Dhruba Tripathi¹, Derek C. Mayne¹, Thomas G. Brown¹

¹University of Calgary, Calgary AB, Canada

ABSTRACT

This paper is focused on understanding the complex phenomenon of ice-structure interaction by the analysis of data from the pressure panels installed on the conical portion of a Confederation Bridge pier. Data from various events of the years 1998 to 2003 were selected for the analysis and evaluation of vertical and horizontal pressure distribution on the conical surface. Out of the 6 rows and 20 columns of pressure panel sectors, considered for analysis, some of the sectors were damaged during installation and others were rendered useless as time passed. Hence, a portion of data had to be omitted during the detailed pressure distribution analysis. The analysis involved the identification of events, pressure peaks, and distribution of pressure peaks on different sectors at different event timestamps. To identify the pressure peaks, a pressure threshold is chosen (for example, 0.2MPa). The pressure peak is the maximum value of pressure reading when it exceeds the threshold. The data is recorded at an interval of 34 milliseconds and to avoid false peaks, caused by electrical interference in the logger system, the pressure peak is considered only when the pressure remains above that threshold for more than 0.34 seconds. Peak pressures were found to occur on the panels at the water-line, reducing with the height above the water-line.

INTRODUCTION

Ice-structure interaction is a complex process in which the ice in the interaction area is highly damaged and the crushed ice is subjected to a complex system of loads and deformations. When ice interacts with a vertical surface, various researchers have found that the ice load is transmitted through discrete areas of intense pressure; the array of high pressure spots can sometimes form a high pressure line (Jordaan, 2001; Daley et al., 1998; Riska et al., 2002). When ice interacts with an inclined structure, the ice force distribution pattern is not so well understood. This paper analyzes data collected from ice force panels (IFPs) installed on the Confederation Bridge pier, P31, to determine the trends and patterns of ice force distribution on the conical surface.

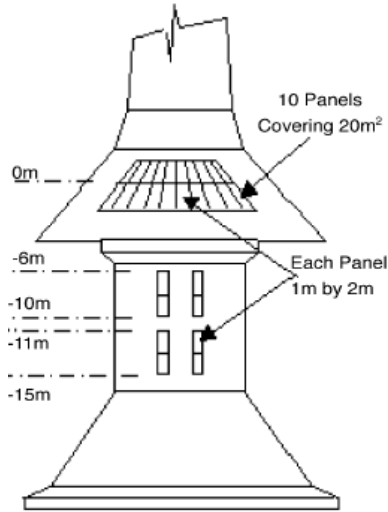


Figure 1. Ice Force Panels layout on the Confederation Bridge pier P31.

INSTRUMENTATION

The IFPs installed in 1996 on the Confederation Bridge pier, as shown in Figure 1, started collecting ice-structure interaction data in 1998 until the panels were damaged by ice in 2003 (Brown et al., 1997, 1998). Figure 2(a) shows 20, 1m x 2m IFPs installed on the conical portion of the bridge pier. The panels were further divided into 8 sectors of an approximate dimension of 0.5m x 0.5m, as shown in Figure 2(b). Approximately, 30 buttons were installed in each sector, two of which were equipped with strain gauge sensors. Hence, the pressure measured by the buttons is not the actual pressure but is only representative of ice pressure on the panels. The pressure results are generally presented in terms of relative pressure, rather than an absolute pressure value. Some of the sectors were rendered non-functional during the installation of panels and others were damaged as time passed. For the analysis, the upper six rows of sectors, where most of the ice structure interaction occurs, are considered. Consequently, there were a total of 76 sectors out of 120 initial sectors that were available for the analysis.

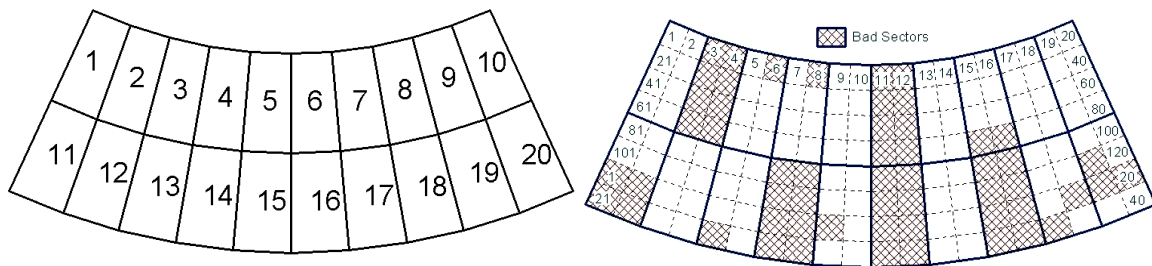


Figure 2. (a) 20 1m x 2m Ice Force Panels (IFPs) arranged in two rows (b) Division of panels into 8 sectors each and indication of bad sectors.

This paper is a part of a research programme in which the distribution of ice pressure on the cone of the bridge pier is investigated (Tripathi et al., 2008). In the initial stage of the work, panel activation analysis was carried out in which the number of sectors activated during an event were counted. However, this analysis failed to register pressure when highly localized ice loads (less

than 78 to 150 mm in diameter) were applied to the panels. These were either missed by the panels or loads were over-predicted depending on the location of application of the localized pressure. The panels could only provide reliable results when ice exerted uniform pressure to the 500 mm x 500 mm sector (Frederking, 1996). This implies that the panel sectors interacting with ice edges might record misleading high pressures and some sectors might not be active even though they seem to be active. Hence, a more detailed analysis for pressure distribution was conducted to obtain actual peaks due to ice loads.

ANALYSIS AND RESULTS

Pressure Peaks Determination

In the detailed pressure distribution analysis, peaks higher than a predefined threshold of 0.2 MPa were identified only when a peak is supported by at least five adjacent values greater than the threshold, both before and after the peak. In other words, the peaks are identified only if the ice pressure greater than the threshold is caused for a minimum of 0.34 seconds, when the time interval between two consecutive readings is 0.034 seconds.

To obtain pressure peaks, a computer program was prepared based on a similar program, used to identify events in tiltmeter data (Tiwari, 2005). The program identifies the pressure peaks registered by each sector over time.

Detailed pressure distribution analysis provides a distribution of peaks in different panel sectors. In a typical pressure history plot for a single sector, Figure 3, peaks are identified by an orange dot on the pressure curve. Such plots are prepared for each sector for each of the selected events.

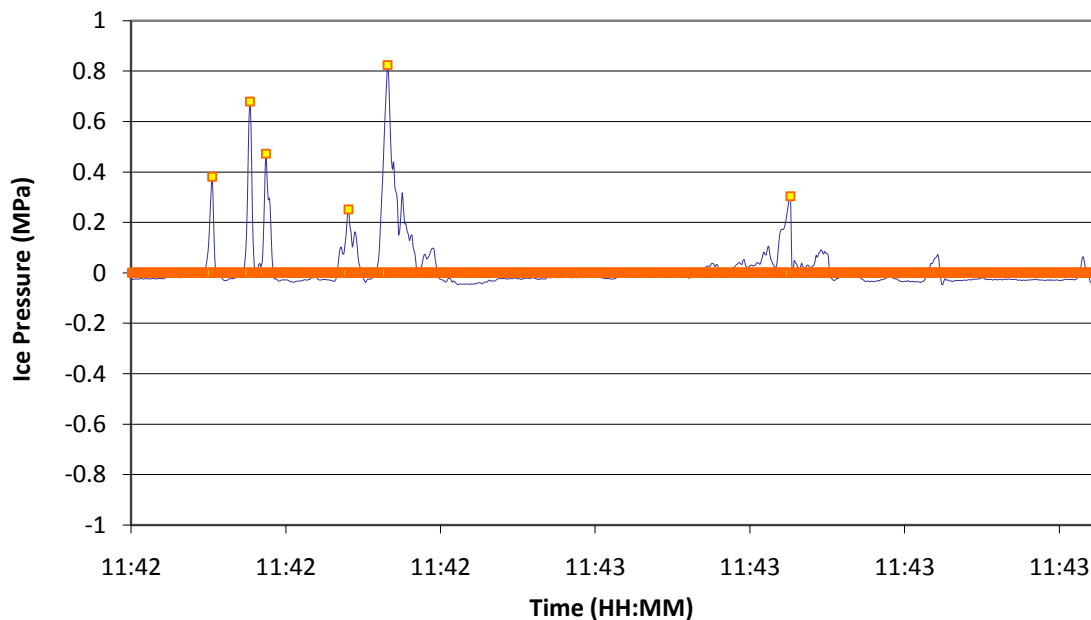


Figure 3. Typical pressure peaks on a sector of the IFP. A peak after the fifth peak is ignored by the algorithm even if the pressure value is greater than 0.2MPa.

To show the overall distribution of ice pressure on the IFP surface, a plot of peak concentration, shown in Figure 4 for the upper six rows of panel sectors, is plotted for each event.

The peak concentration (PC_i) is computed by the relationship given by Equation 1.

$$PC_i = \frac{P_i}{\sum_{j=1}^{ng} P_j} \times 100 \quad (1)$$

Where, P_i is the number of peaks on a sector i during an event and P_j is the number of data in ng good sectors.

To simplify the concentration plot, bar charts are plotted on each sector on the plot grid representing the actual layout of the IFPs. Each individual bar in the bar plot represents PC_i of 0.5%. These bars are color coded for the differentiation of high and low concentration of ice pressure. Bar plots with PC_i value greater than 5 percent are trimmed to prevent overflow of the plot to another sector.

Bars for $PC_i > 3.0\%$ are plotted in red (■), bars for $1.0 < PC_i < 3.0\%$ are plotted in black (■) and, bars representing $PC_i < 1.0\%$ are plotted in blue (■). The blank (not shaded) sectors are bad sectors and the lightly shaded sectors didn't see ice pressure during the event.

Rows/Columns

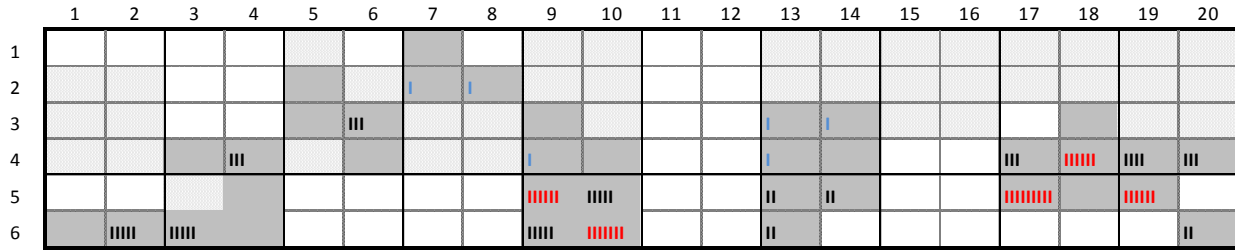


Figure 4. Typical distribution of ice pressure on pressure panel sectors (Each bars representing peak concentration (PC_i) of 0.5%, white box are sectors either without ice pressure or bad sector).

Yearly Distribution of Pressure

To assess the annual distribution of pressure peaks, the peak frequency percentage is calculated by dividing the total number of peaks in a sector, in a year, by the total number of peaks in all the ice force panel sectors.

The peak frequency (PF_i) is computed by the relationship given by Equation 2.

$$PF_i = \frac{YP_i}{N} \times 100 \quad (2)$$

Where, YP_i is the number of peaks on the sector i in an event and N is the total number of data in the year.

To normalize the peak frequency in the active sectors, weighted average frequency is calculated by the relationship given by Equation 3. These peak frequencies are plotted for all years as shown in Figure 5.

The Weighted Average Frequency (WAF_i) is computed by the following equation:

$$WAF_i = \frac{PF_i \times N_{ri}}{T_{NS}} \quad (3)$$

Where, PF_i is obtained from Equation 2, N_{ri} is the total number of sectors in the row i , and T_{NS} is the total numbers of good sectors.

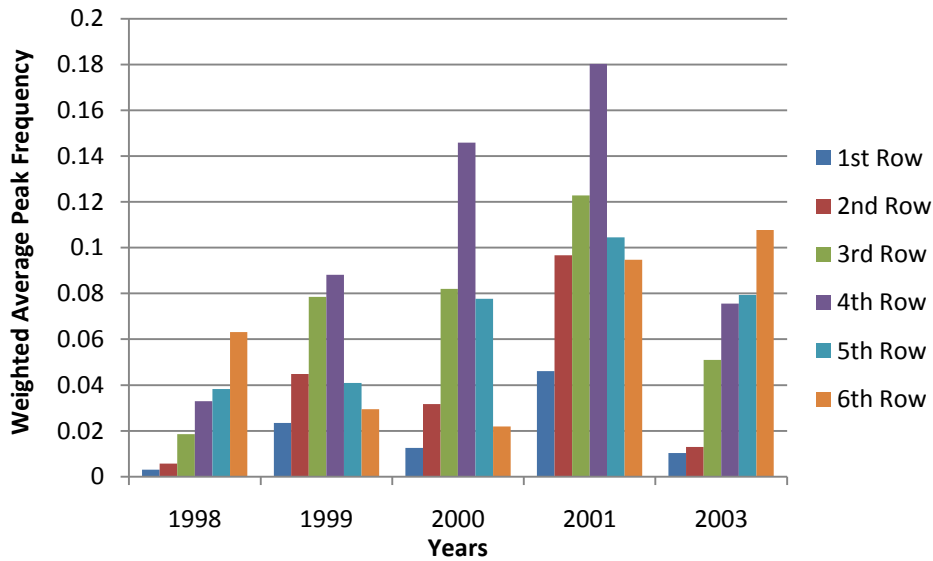


Figure 5. Annual distribution of pressure peaks on each row (Rows 1-6 from top to bottom).

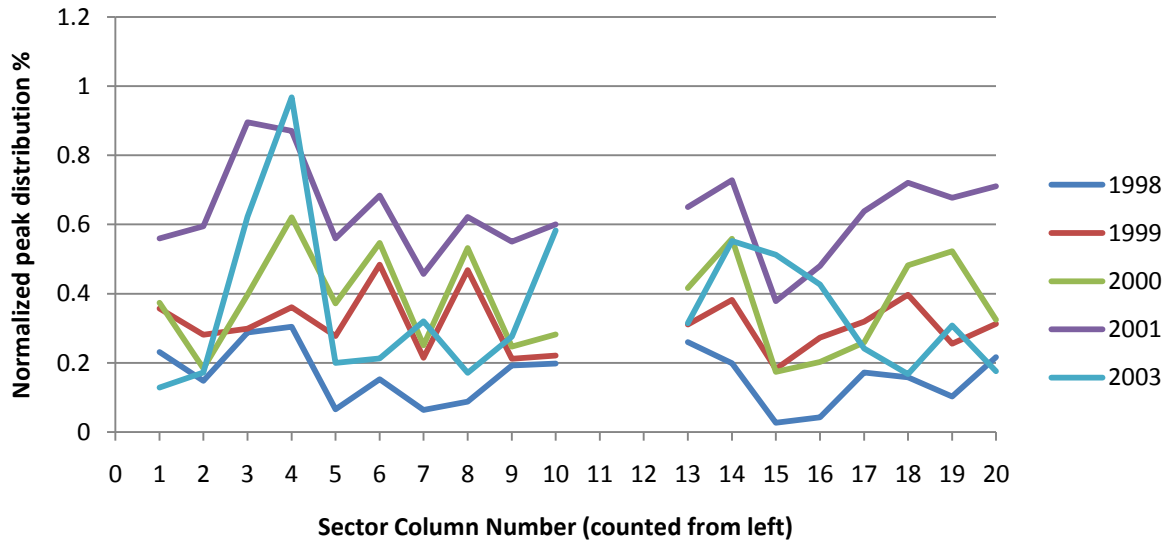


Figure 6. Horizontal distribution of pressure on the top six rows of pressure panel sectors (Columns 1-20) from left to right.

The vertical distribution of the pressure was obtained for row numbers 1 to 6 from top to bottom of the pressure panel. The top of the panels is 1.6 m. above mean water level and hence receives rubble piles rather than the ice sheet. These panels typically receive the least amount of ice pressure. As we go downwards, the ice pressure and hence, the peak frequency starts to increase until we reach the 5th row, at the waterline. Then on the sixth row, the pressure value decreases. This pattern confirms the common logic that the ice pressure at the water line is highest and it starts to decrease as we go away from the water line.

The pattern and amount of such distribution of pressure peaks however is not consistent in different years.

In a similar manner, the horizontal distribution of peaks in a row of sectors is obtained by calculating the normalized peak percentage for each column of sectors, 1 to 20, starting from the left end. Figure 6 shows a distribution that doesn't follow any definite pattern. In contrast to the vertical distribution, the horizontal distributions were more severely affected by the existence of a bad sector in a column. For example, there were three bad sectors in column No. 2, hence the normalized peak was low compared to the first column. Two columns, 11 and 12, didn't have any good sectors; hence there is a gap at the center of Figure 6. Having damaged sectors at the waterline is one of the reasons for the skew in the horizontal distribution of pressure. For example, bad sectors in column numbers 7, 8, 15, 16, and 19 (Figure 2, b) are at the mean waterline, causing low pressure peak distribution in the respective columns.

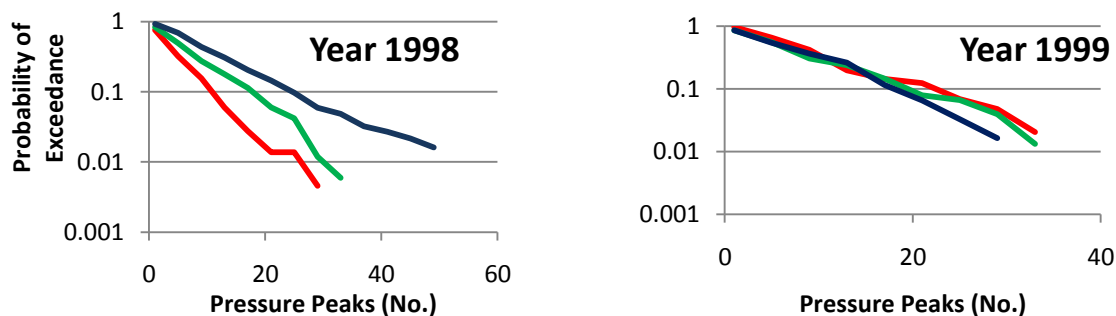
The Probability of Exceedance

The probability of exceedance of pressure peaks on the pressure panel sector is calculated by the Equation 4.

$$\text{Probability of Exceedance} = 1 - \left[X_{(i-1)} + \frac{x_i}{\sum x_i} \right] \quad (4)$$

Where, x_i is the pressure peak frequency of a sector i in a year.

Aggregate probability of exceedance of pressure peaks for the years 1998, 1999, 2000, 2001 and 2003 are plotted (Figure 7) for three different rows of pressure panel sectors at the waterline. In the figure, the red line represents sectors in the row above mean water level, the blue line represents the sector row below the mean water level and the green line represents the sectors at the mean water level.



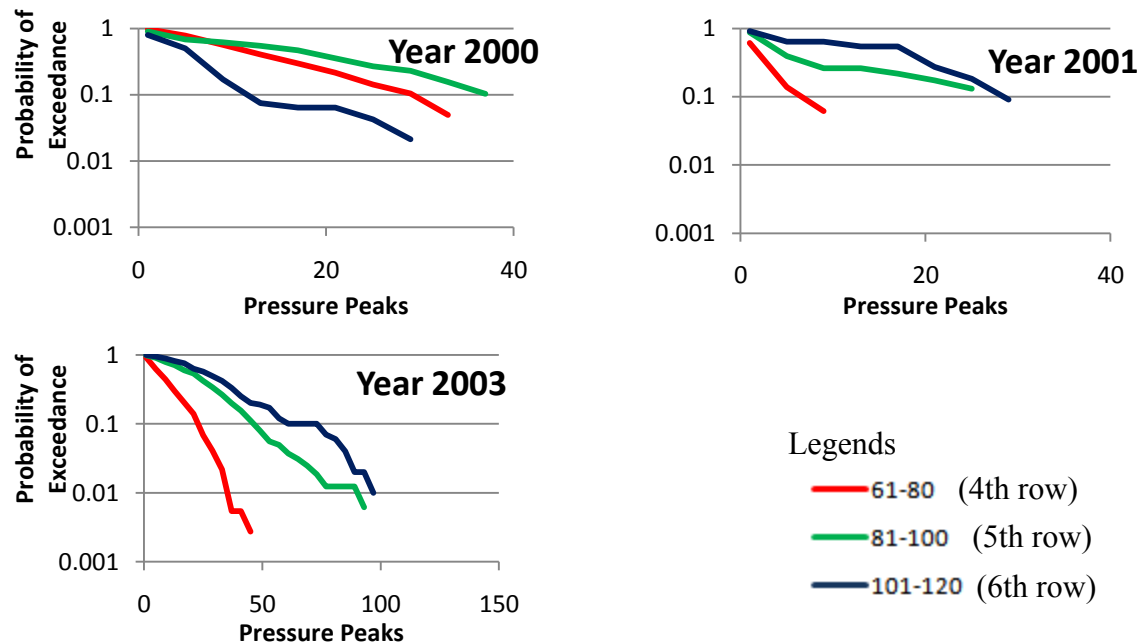


Figure 7. Probability of exceedance of pressure peak frequencies for the years 1998, 1999, 2000, 2001, and 2003 on three rows near the mean water-line.

The plots in Figure 7 show considerable scatter but a pattern can be seen in some years. In years 1998, 2001, and 2003 the trend seen is as expected: the lower sector row (sixth row with sectors 101-120) having the highest distribution of pressures, and the higher sectors (fourth row with sector 61- 80) having the lowest distribution. In 1999, all the three rows of panels exhibit approximately the same pressure distribution, while in 2000, the middle row of panels exhibit the highest pressure distribution.

The mean water line approximately coincides with the boundary between the lower sector row (sectors 101-120) and the middle row (sectors 81-100). The tidal range is approximately ± 0.7 m and each sector corresponds to a vertical distance of 0.39m. Accordingly, one would expect that the lower panels would experience the greater number and magnitude of pressure peaks, as they are more likely to encounter the incoming intact level ice, whereas, sectors further up the cone are more likely to encounter rubble ice.

RESULTS

It is seen that the pressure is concentrated on and around the mean waterline where level ice interacts with the pier. Depending on the tidal level, the ice pressure concentration is observed to change in the vertical direction. The ice pressure caused by the ice rubble is found to be less than that of the level ice and hence the pressure distribution decreases with height above the mean waterline. The ice rubble pressure on an inclined structure is mainly caused by its surcharge weight whereas, the pressure at the ice-structure interface at the water level is caused by the ice breaking force and the forces required to push the sheet up the slope, through the ice rubble.

Hence, the vertical pressure distribution in Figure 5 shows the decreasing trend in pressure above the fourth row of the panel sector.

The distribution of ice pressure on the horizontal direction (Figure 6) exhibits much scatter and no obvious pattern can be observed in the yearly distribution. One might expect to see higher pressure in the central portion of the IFPs but, there is no data to support it. Distribution of pressure around the perimeter of the cone is based on the data obtained from six sectors in each column of panel sectors and having one or more bad sectors in half of them significantly reduces the reliability of the results. Having a damaged sector at the waterline is another factor to cause error in distribution. In general, the yearly distribution is more or less constant in the horizontal direction. Unlike the vertical distribution, where the ice impact pattern differs from water level and away from water level, the horizontal distribution averages out when long-term data are considered. More evident distributions are obtained when distribution of pressure is obtained for an individual event which is beyond the scope of this paper.

Although the pressure panels on the Confederation Bridge couldn't give absolute ice pressure, they have proved to be good enough to give insights in the distribution pattern of ice pressure at the ice-structure interface.

CONCLUSION

The pressure panels installed on the bridge pier were designed such that they were only good in obtaining the pressure distribution rather than absolute pressure. Hence, the attempt was done to obtain the pressure distribution on the panel surface. Some of the panel sectors were damaged during the installation and some more were damaged later, hence a complete spatial distribution couldn't be obtained due to the unavailability of data from all the sectors.

- The pressure in the vertical direction of the pressure panel assembly decreases both above water-line and below waterline
- The horizontal distribution of pressure is less distinct largely because of fewer numbers of sectors in each column. The panels in the central portion of the panel assembly were damaged and some of the other sectors at the water-line were also damaged.
- The probability of exceedance plots reinforces the vertical pressure distribution on the pressure panel.

Although out of the scope of this paper, similar trend of pressure distribution was observed in activation analysis and correlation analysis. These data coupled with the activation analysis, correlation analysis, and video data analysis will complement to form a more detailed ice-pressure distribution on offshore inclined structures.

ACKNOWLEDGEMENT

The authors would like to acknowledge the support of Strait Crossing Bridge Ltd., Public Works and Government Services Canada, the National Science and Engineering Research Council (NSERC) and NRC-Canadian Hydraulics Centre.

REFERENCE

- Brown, T. G., Croasdale, K.R. (1997). Confederation Bridge Ice Force Monitoring Joint Industry Project Annual Report - 1997, IFN Engineering Ltd.
- Brown, T. G. (2006). Confederation Bridge – An innovative approach to ice forces. The 2006 Annual Conference of the Transportation Association of Canada, Charlottetown, Canada.
- Brown, T. G., Bruce, J. R., Croasdale, K.R. (1998). Confederation Bridge Ice Force Monitoring Joint Industry Project Annual Report - 1998, IFN Engineering Ltd.
- Daley, C., Tuhkuri, J., Riska, K. (1998). The role of discrete failures in local ice loads. Cold Regions Science and Technology 27: 197-211.
- Frederking, R. (1996). IFP Calibration Report, National Research Council of Canada.
- Jordaan, I. J. (2001). Mechanics of Ice-Structure Interaction. Engineering Fracture Mechanics 68: 1923-1960.
- Riska, K., Uto, S., Tuhkuri, J. (2002). Pressure distribution and response of multiplate panels under ice loading. Cold Regions Science and Technology 34: 209-225.
- Tiwari, D. (2005). Information Management in Monitoring of the Confederation Bridge for Ice Force Issues. M.Sc. Thesis, Department of Civil Engineering. Calgary, University of Calgary.
- Tripathi, D., Brown, T. G. and Mayne, D. C. (2008). Ice Pressure Distribution during Ice-Structure Interaction: Measurements of Ice Force Panels on Confederation Bridge Pier. Proceedings of the 19th IAHR International Symposium on Ice, Vancouver, Canada, pp. 737-749.